

EFFECTS OF RECLAMATION PROJECT ON WATER ENVIRONMENT IN STRONG TIDE ESTUARY

Yongjun LU & Haolin LI
Nanjing Hydraulic Research Institute, Nanjing 210029, China

Abstract: A 2-D tidal current and sediment mathematical model has been developed according to the characters of strong tide estuary in the Oujiang Estuary and Wenzhou Bay, i.e. complicated boundaries, multi-islands, existence of turbidity and significant difference of the size distribution of bed material along. The governing equations based on boundary-fitted grid with orthogonal curvilinear coordinate for non-uniform suspended load and bed load are introduced. The numerical solutions, initial conditions, boundary conditions and movable boundary techniques are presented. The solutions of some problems in calculations, such as critical condition of deposition or erosion, sediment carrying capacity, non-uniform bed load transport rate etc. are suggested. The calculated tidal levels are in a good agreement with the measured ones in the 18 tidal level stations. The calculated velocities and flow directions still fit well with the measured values among the total 52 observed synchronous vertical lines distributed in 8 cross sections. The calculated input and output tidal discharges through Huangda'ao section are rather close to those measured. And the calculated values of bed deformation in the both reaches from Yangfushan to the estuary outfall and out-sea area are in a good agreement with the observed from 1986 to 1992. By using this model, the changes of tidal influx through the estuary, velocities in different channels and the bed changes are predicted respectively under the influence of reclamation project in the Wenzhou shoal.

Key words: Strong tide estuary, Reclamation project, Water environment, Mathematical model, Tidal current, Non-uniform suspended load, Non-uniform bed load, Bed deformation

1. INTRODUCTION

Development and application of hydrodynamic models to predict flow and sediment transport in estuarine, coastal, and shelf waters has been extremely active over the past two decades (Spaulding et al. 1994), most of these studies employing well known finite-difference techniques on a rectangular grid. Although this has been proven useful in various applications, it becomes expensive when the study region is geometrically and/or bathymetrically complex. The numerical truncation error is most evident for narrow river reaches where the lateral resolution is handled by only a few grids (Muin et al. , 1996). Computational resolution costs prevent further refinement of the grid resolution for these areas. Such difficulties have motivated the introduction of curvilinear coordinate transformations (Johnson, 1980; Sheng, 1986; Baber, 1992; Willemse et al. , 1985).

At present, several 2D tidal models for estuaries are available. Muin and Spaulding (1996) developed a 2D model by use of a non-orthogonal boundary-fitted technique for predicting sea level and current. Shaoling and Kot (1997) proposed a 2D simulation of tides in the Pearl River estuary with a moving boundary. Kelin Hu et al. (2000) suggested a 2D current field model integrating the Yangtze Estuary with the Hangzhou Bay. Dou et al. (2000) presented a 2D numerical model of total uniform sediment transport in the Yangtze Estuary.

This paper is to present a model for simulation of the tidal current and sediment transport in the Oujiang Estuary and the Wenzhou Bay, which have a complicated boundary with multiple

islands, and are influenced by both runoff and tidal current, both suspended load and bed load, and both clear water and turbid water. By using this model, the changes of tidal influx through the estuary, velocities in different channels and the bed changes are predicted respectively under the influence of reclamation project in the Wenzhou shoal.

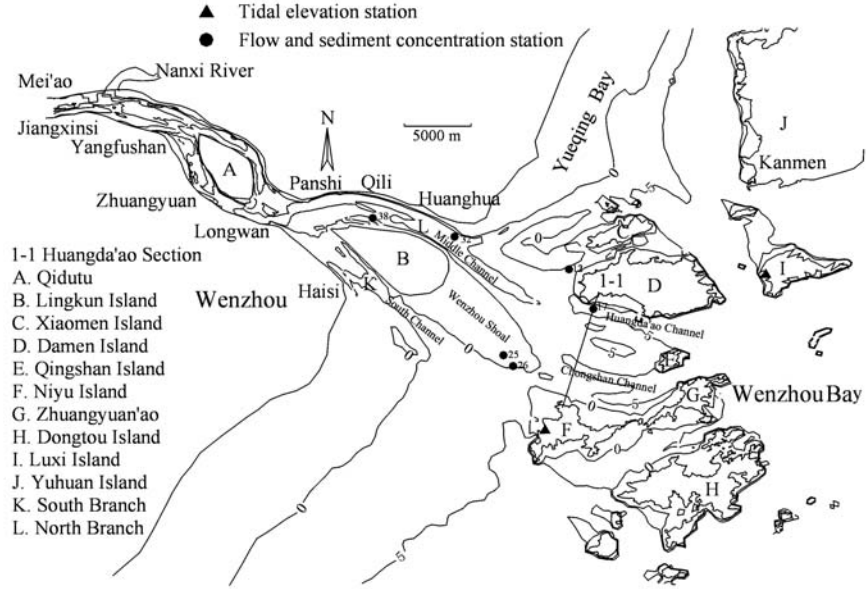


Fig. 1 Sketch of Oujiang Estuary

2. GOVERNING EQUATIONS

Computational difficulties in natural water body, such as irregular boundary figures, great disparity between length and width of calculated area, etc. can be overcome by using the boundary-fitting orthogonal coordinate system. Generating a grid in an arbitrary physical domain involves a coordinate transformation from the physical plane (x, y) to the computational plane (ξ, η) . This is done by solving a system of Poisson equation (Willemse, 1986). Water Flow Equation includes Continuity equation, Momentum equation in ξ direction and Momentum equation in η direction (Lu, 1998).

2.1 NON-EQUILIBRIUM TRANSPORT EQUATION FOR NON-UNIFORM SUSPENDED LOAD

The non-uniform suspended load is divided into n_0 groups. Let, S_L be the concentration of group L, P_{SL} be the percent of the Lth group. Then

$$S_L = P_{SL} S, \quad S = \sum_{L=1}^{n_0} S_L$$

where, S is the total concentration of suspended load. The 2-D depth-averaged un-equilibrium transport equation is

$$\begin{aligned} \frac{\partial h S_L}{\partial t} + \frac{1}{C_\xi C_\eta} \left[\frac{\partial}{\partial \xi} (C_\eta h u S_L) + \frac{\partial}{\partial \eta} (C_\xi h v S_L) \right] = \\ \frac{1}{C_\xi C_\eta} \left[\frac{\partial}{\partial \xi} \left(\frac{\varepsilon_\xi}{\sigma_s} \frac{C_\eta}{C_\xi} \frac{\partial h S_L}{\partial \xi} \right) + \frac{\partial}{\partial \eta} \left(\frac{\varepsilon_\eta}{\sigma_s} \frac{C_\xi}{C_\eta} \frac{\partial h S_L}{\partial \eta} \right) \right] + \alpha_L \omega_L (S_L^* - S_L) \end{aligned} \quad (1)$$

in which, S_L^* = suspended load carrying capacity of the group L, $S_L^* = P_{SL}^* S^*(\omega)$; P_{SL}^* = fractional percent of carrying capacity of the group L; $S^*(\omega)$ = carrying capacity of total

suspended load; α_L =suspended load recovery coefficient for size-class L ; ω_L = the fall velocity of the group L , $\omega_L=0.015$ cm/s for $D_L \leq 0.015$ mm and

$$\omega_L = \sqrt{\left(13.95 \frac{v}{D_L}\right)^2 + 1.09 \frac{\rho_s - \rho}{\rho} g D_L - 13.95 \frac{v}{D_L}} \quad \text{for } D_L > 0.015 \text{mm}$$

$\varepsilon_\xi, \varepsilon_\eta$ = diffusion coefficient of suspended load in the ξ, η direction. It is assumed that $\varepsilon_\xi, \varepsilon_\eta = v_t; \sigma_s = 1$.

2.2 NON-EQUILIBRIUM TRANSPORT EQUATION FOR NON-UNIFORM BED LOAD

The non-uniform bed load is divided into n_b groups. Dou's (2001) 2-D depth-averaged non-equilibrium transport equation is as follows:

$$\begin{aligned} \frac{\partial h S_{bL}}{\partial t} + \frac{1}{C_\xi C_\eta} \left[\frac{\partial}{\partial \xi} (C_\eta h u S_{bL}) + \frac{\partial}{\partial \eta} (C_\xi h v S_{bL}) \right] = \\ \frac{1}{C_\xi C_\eta} \left[\frac{\partial}{\partial \xi} \left(\frac{\varepsilon_\xi}{\sigma_b} \frac{C_\eta}{C_\xi} \frac{\partial h S_{bL}}{\partial \xi} \right) + \frac{\partial}{\partial \eta} \left(\frac{\varepsilon_\eta}{\sigma_b} \frac{C_\xi}{C_\eta} \frac{\partial h S_{bL}}{\partial \eta} \right) \right] + \alpha_{bL} \omega_{bL} (S_{bL}^* - S_{bL}) \end{aligned} \quad (2)$$

in which, S_{bL}^* =concentration of bed load transport capacity along total depth for size-class L ; $S_{bL}^* = g_{bL}^* / \left(\sqrt{u^2 + v^2} h \right)$, g_{bL}^* =unit-width bed load transport rate; S_{bL} = concentration of bed load transport along total depth for size-class L . $S_{bL} = g_{bL} / \left(\sqrt{u^2 + v^2} h \right)$; α_{bL} =bed load recovery coefficient for size-class L ; ω_L = the fall velocity of the group L ; $\sigma_b = 1$.

2.3 SORTING EQUATION OF BED MATERIAL (RAHUEL AND HOLLY ET AL 1989; HOLLY AND RAHUEL, 1990)

Each sediment size class L has a mixed-layer mass-conservation equation as follows:

$$\begin{aligned} \gamma_s \frac{\partial E_m P_{mL}}{\partial t} + \alpha_L \omega_L (S_L - S_L^*) + \alpha_{bL} \omega_{bL} (S_{bL} - S_{bL}^*) + \\ [\varepsilon_1 P_{mL} + (1 - \varepsilon_1) P_{mL0}] \gamma_s' \left(\frac{\partial Z_L}{\partial t} - \frac{\partial E_m}{\partial t} \right) = 0 \end{aligned} \quad (3)$$

In equation (8), γ_s, γ_s' = unit weight of sediment and dry unit weight of deposited sediment respectively; P_{mL0} = fractional representation of size-class L in the initial bed material; P_{mL} = fractional representation of size-class L in the mixed layer; E_m = thickness of the mixed layer; $\varepsilon_1 = 0$ or 1 for mixed-layer floor descending or rising, respectively.

2.4 CHANNEL BED DEFORMATION EQUATION

$$\gamma_s \frac{\partial Z_L}{\partial t} = \alpha_L \omega_L (S_L - S_L^*) + \alpha_{bL} \omega_{bL} (S_{bL} - S_{bL}^*) \quad (4)$$

where, Z_L = the thickness of erosion or deposition for the L th group. The total thickness of erosion or deposition $Z = \sum_{L=1}^n Z_L$.

3. NUMERICAL SCHEME AND NUMERICAL SOLUTION

It is found that the structure of water flow equation and equation (1-2) is similar and can be generalized as follows

$$C_\xi C_\eta \frac{\partial \psi}{\partial t} + \frac{\partial (C_\eta u \psi)}{\partial \xi} + \frac{\partial (C_\xi v \psi)}{\partial \eta} = \frac{\partial}{\partial \xi} \left(\Gamma \frac{C_\eta}{C_\xi} \frac{\partial \psi}{\partial \xi} \right) + \frac{\partial}{\partial \eta} \left(\Gamma \frac{C_\xi}{C_\eta} \frac{\partial \psi}{\partial \eta} \right) + C \quad (5)$$

where, $\psi = H, u, v, S_L$ or S_{bL} ; Γ = diffusion coefficient; C = sources. The equation(5) is

solved by use of the control volume method.

A staggered grid system is used where the control volume for u and v are centered on the faces of the control volume for the scalar variables, h , S , g_b and Z are located at the center of the continuity control volume, which is known to suppress the wiggles or the checkboard patterns of the pressure.

Eq.(10) is formally the same as the general governing equation derived in Cartesian coordinates. Because of this similarity, the Patarkar—Spalading's SIMPLEC solution procedure which has been successfully used for flow computation in Cartesian coordinates, can be extended to the numerically simulation in the present orthogonal curvilinear coordinate system without any modifications, as was discussed by Lu (1998). The power law scheme is used to discretize Eq. (5). The details of the calculation were presented in Ref. (Lu, 1998).

4. INITIAL CONDITIONS, BOUNDARY CONDITIONS AND MOVABLE BOUNDARY TECHNIQUE

4.1 INITIAL CONDITIONS

The initial water level is set to the average of tidal levels observed on the computational boundary. The initial tidal velocity is taken as zero. The initial sediment concentration is taken from interpolation of field data.

$$\begin{aligned} H(\xi, \eta)|_{t=0} &= H_0(\xi, \eta) & u(\xi, \eta)|_{t=0} &= 0 \\ v(\xi, \eta)|_{t=0} &= 0 & S_L(\xi, \eta)|_{t=0} &= S_{0L}(\xi, \eta) \end{aligned}$$

4.2 BOUNDARY CONDITIONS

The upstream boundary condition is field measured flow hydrograph at Weiren station:

$$Q = Q(t)$$

On the open sea boundary, the water level is prescribed based on field data:

$$H = H(t)$$

The relationship between sediment concentration and flow discharge at Weiren station is extracted from the field data.

$$\begin{aligned} S &= 4 \times 10^{-4} Q^{0.5242} & \text{for } Q \leq 500 & \text{ m}^3/\text{s} \\ S &= 3 \times 10^{-7} Q^{1.7058} & \text{for } Q > 500 & \text{ m}^3/\text{s} \end{aligned}$$

The concentration of 0.16 kg/m^3 is assigned to the open sea boundary.

4.3 MOVABLE BOUNDARY TECHNIQUE

In unsteady flow simulation, a part of bed may be exposed to air due to water level dropping. To deal with the change of computation domain, a moving boundary technique is used. Via imposing very large roughness on the computational cells exposed to the air, the velocities in cells tend to be zero.

5. TREATMENT OF KEY PROBLEMS IN COMPUTATION

5.1 CRITICAL CONDITIONS FOR EROSION AND DEPOSITION

The comparison between sediment concentration (S) and sediment transport capacity by weight (S^*) is used as the criterion for erosion and deposition: if $S > S^*$, deposition will occur, or otherwise, if $S \leq S^*$, erosion will take place for $V \geq V_c$, and a regime state will result for $V < V_c$, where V_c is the incipient velocity of sediment.

In this study, different formulas for determination of the incipient velocity are employed based on the features of local sediment. Inside the Oujiang Estuary, Dou's formula (Dou, 2000) is used:

$$V_{cl} = k \left(\ln 11 \frac{h}{\Delta} \right) \left(\frac{d'}{d_*} \right)^{\frac{1}{6}} \sqrt{3.6 \frac{\rho_s - \rho}{\rho} g D_L + \left(\frac{\gamma_0}{\gamma_{0*}} \right)^{\frac{1}{2}} \frac{\varepsilon_0 + gh\delta(\delta / D_L)^{\frac{1}{2}}}{D_L}} \quad (6)$$

in which, h is water depth, D_L median diameter of the L-th group, Δ roughness height, ρ_s and ρ are water and sediment density respectively, g is gravitational acceleration, γ_0 dry unit weight, γ_{0*} stable dry unit weight, ε_0 synthetic parameter of cohesive force, and δ parameter of water film thickness. The values of the parameters used herein are: $k' = 0.32$, $\Delta = 1.0$ mm, $d' = 0.5$ mm, $d_* = 10$ mm, $\gamma_0 = 1750d^{0.183}$, $\varepsilon_0 = 1.75$ cm/s² for natural sediment, and $\delta = 2.31 \times 10^{-5}$ cm.

Outside the Oujiang Estuary Tang's formula (Tang, 1963) is used.

$$V_c = \frac{m}{m+1} \left(\frac{h}{D_L} \right)^{\frac{1}{m}} \sqrt{3.2 \frac{\gamma_s - \gamma}{\gamma} g D_L + \left(\frac{\gamma'}{\gamma'_0} \right)^{10} \frac{C}{\rho D_L}} \quad (7)$$

in which, γ'_0 is stable wet unit weight and $\gamma'_0 = 1.6$ g/cm³; γ' unit weight and $\gamma' = 1.2 \sim 1.4$ g/cm³; $m=6$.

5.2 SUSPENDED LOAD TRANSPORT CAPACITY

The concept of background concentration (S_0) is introduced. The formula of sediment transport capacity results from regression of the field data.

$$S^* = k_0 \frac{V^2}{gh} + S_0 \quad (8)$$

where the values of k_0 and S_0 are listed in Table 1.

Table 1 The values of k_0 and S_0 for different zones

| Zone | k_0 | S_0 |
|--------------------------|--------|--------|
| Jiangxinsi~Panshi(I) | 14.132 | 1.4302 |
| Outfall of Oujaing(II) | 8.487 | 0.5415 |
| Outside Oujiang(III) | 2.617 | 0.1672 |
| Yueqing Bay(IV) | 0.470 | 0.1500 |

5.3 DISCHARGE OF NON-UNIFORM BED LOAD

A formula of non-uniform bed load discharge based on the concept of flow power has been developed by Lu (Lu and Zhang, 1992)

$$g_{bL} = K_b \frac{\gamma_s}{\gamma_s - \gamma} \tau_0 u_* P_{mL} [1 - 0.7 \sqrt{\frac{\theta_{crL}}{\theta_L}}] (1 - q_L) \quad (9)$$

in which, $\tau_0 = \gamma R J$; $u_* = \sqrt{\tau_0 / \rho}$; ρ is water density; q_L is the probability that the particals of D_L remain on the top layer and it can be determined by modified Gessler's formula

$$q_L = 1 - \frac{1}{\sigma \sqrt{2\pi}} \int_{-\infty}^{\xi_L} \frac{0.031(\gamma_s - \gamma) D_L}{\tau} \exp\left(-\frac{t^2}{2\sigma^2}\right) dt \quad (10)$$

$$\text{where, } \xi_L = \begin{cases} 10^{0.55 \lg^2(D_L / D_m) - 0.204 \lg(D_L / D_m) - 0.112} & (D_L \leq 0.5 D_m) \\ 0.895 (D_L / D_m)^{-0.16} & (D_L > 0.5 D_m) \end{cases} \quad (11)$$

and the critical Shields' number is

$$\theta_{crL} = 0.031 \xi_L$$

$$\theta_L = \tau_0 / [(\gamma_s - \gamma) D_L]$$

The coefficient K_b in equation (9) is determined by experimental data. Declining of the discharge in the process of armoring can be reflected by K_b (Lu *et al.*, 1998).

$$K_b = \begin{cases} 11.6 & (\theta > 0.25) \\ 10^{0.2256 - 2.534 \lg \theta - 1.896 \lg^2 \theta} & (0.06 < \theta < 0.25) \\ 10^{12.8719} \theta^{10.1319} & (\theta \leq 0.06) \end{cases}$$

6. MODEL VERIFICATION

6.1 COMPUTATION DOMAIN AND ITS DISCRETIZATION

The upstream boundary of the model is taken at the Weiren hydrometric station, about 45 km upstream away from Wenzhou. The sea boundary is on the connecting line from Feiyunjiang Estuary through Nanji Island to Kanmen (including the Yueqing Bay). The model covers an area of about 4500 km².

For the bathymetry in the model, the 1/25000 scale chart is used outside the Oujiang Estuary and the Yueqing Bay, while 1/10000 inside the Oujiang River. The total number of grid nodes is 319 in the current direction and 131 in its orthogonal direction. The grid lines usually intersect at 89–92° except some nodes close to the boundary. The grid sizes are 100–200 m, 300–600 m, and 100–500 m for the Oujiang River, the outer sea, and the area between them, respectively.

6.2 VERIFICATION OF TIDAL CURRENT

The first synchronous hydrometric measurement was conducted from Oct. 10 to 12, 1999, the second from Oct. 12 to 13, 1999, and the third from Oct. 14 to 15, 1999. The measuring points are shown in Fig. 1. The tidal level curve for the connecting line from Feiyunjiang Estuary (Shangguan mountain) through Nanji Island to Kanmen is adjusted in computation, so that the computational results for the total 52 verticals, including velocity, flow direction and flow rate through Huangda'ao cross section, can be in good agreement with the field data. Figs. 2 and 3 show the comparison between the computational results and the fields data of the first synchronous measurement. The roughness 0.021 is taken for the Oujiang River due to the coarser bed material; 0.016 for the Yueqing Bay and 0.014 for the outer sea because of the finer bed material there.

As shown in Fig.2, the computed tidal level is consistent with the observed data in both magnitude and phase, the deviation being is within 0.1m. The computed velocity and flow direction are also in good agreement with the field data in both magnitude and phase (Fig. 3).

The computed and measured tidal discharges through Huangda'ao cross section are plotted in Fig. 4. The computed discharge is close to the field data in both magnitude and phase.

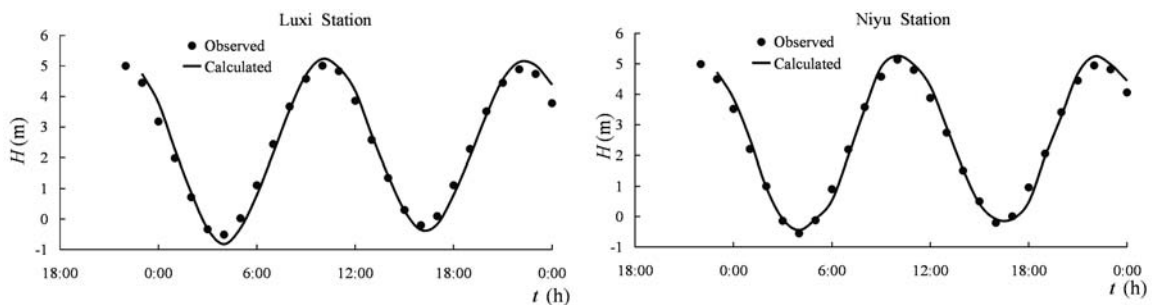


Fig. 2 Tidal level verification against the first synchronous measurement (spring tide)

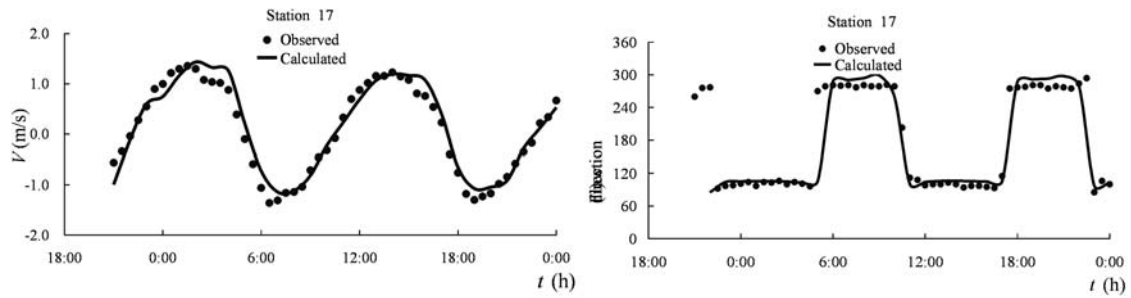


Fig. 3 Tidal current verification against the first synchronous measurement (spring tide)

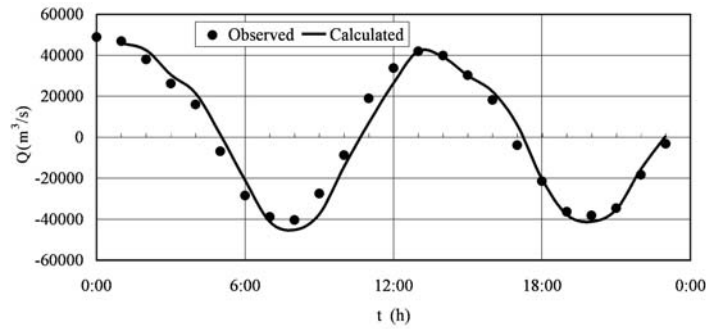


Fig. 4 Verification of tidal discharge through Huangda'ao cross section (1999.10.11-12)

6.3 VERIFICATION OF SUSPENDED LOAD CONCENTRATION

The suspended load is composed of 5 groups whose diameters range from 0.003mm to 0.175mm. The bed deformation induced by the size group of $d=0.375-12.5\text{mm}$ is mainly due to bed load transport.

Fig.5 shows the comparison of computed results with the field data measured in the first and third synchronous measurements. As shown in this figure, the computed concentration hydrographs are in basic agreement with the field data. The results suggest the general pattern of sediment transport in the Oujiang Estuary, that is, during flood tide, the sea water enters the river, the velocity and transport capacity increase along distance, and the sediment concentration is relatively high; during ebb tide, the turbid water from the Jiangxinsi-Longwan reach flows into the sea, the velocity and transport capacity decrease, and the sediment concentration is then reduced.

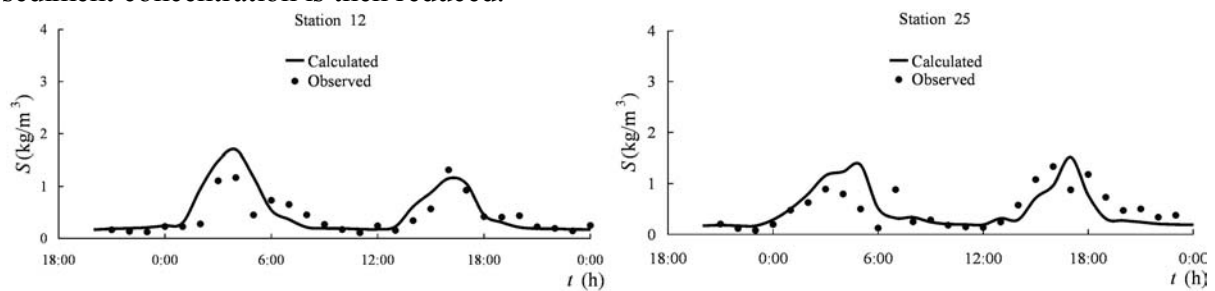


Fig. 5a Verification of sediment concentration against the first synchronous measurement (spring tide)

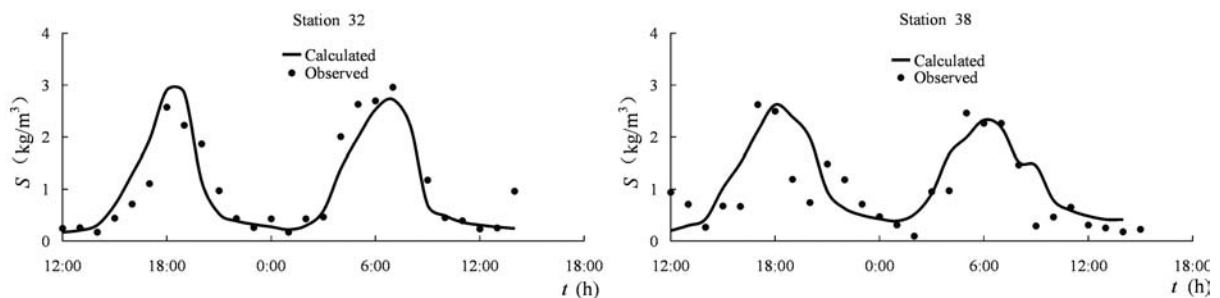


Fig. 5b Verification of sediment concentration against the third synchronous measurement (neap tide)

6.4 VERIFICATION OF BED DEFORMATION

The hydrologic processes at Weiren station in 1987–1992 is used as the typical hydrologic series and the discharge hydrograph is generalized. A series of spring, moderate and neap tides on the connecting line from Shangguan mountain through Nanji island to Kanmen is assembled as the typical tides. The bathymetry surveyed in Oct., 1986 is used as initial bed form, and the computation is carried out for a period of time from Oct. 1986 to Oct. 1992. The computed and observed erosion and deposition for different reaches from Yanfushan to the outfall are listed in Table 2. From this table, it can be seen that the volume of observed and computed erosion amounts is respectively $16.997 \times 10^6 \text{ m}^3$ and $14.613 \times 10^6 \text{ m}^3$ for the reach from Jiangxinsi to the downstream side of Qidu, and $2.321 \times 10^6 \text{ m}^3$ and $2.672 \times 10^6 \text{ m}^3$ for the reach from the downstream side of Qidu to the upstream side of Lingkun. The observed and the computed deposition around Lingkun Island is $2.452 \times 10^6 \text{ m}^3$ and $1.647 \times 10^6 \text{ m}^3$, respectively. The computed erosion and deposition are in good agreement with the field-data.

Table 2 Erosion and deposition for different reaches from 1986 to 1992 (10^6 m^3)

| Reach | computed | observed |
|--|----------|----------|
| Jiangxinsi–the downstream side of Qidu | -14.613 | -16.997 |
| the downstream side of Qidu–the upstream side of Lingkun | -2.672 | -2.321 |
| Lingkun Island | 1.647 | 2.452 |

Note: “-” refers to erosion, “+” deposition.

The results of verification show that the generalization of the stream flow and the tidal process in the outer sea is reasonable, and the determination of sediment transport capacity and sediment concentration recovery coefficient and the criterion of erosion and deposition are all correct. Therefore, the model can be used to predict bed deformation in the Oujiang Estuary.

7. APPLICATION

The model has been applied to the prediction of the changes of tidal volume, flow velocity and bed deformation in the Oujiang Estuary, resulting from the reclamation project in the Wenzhou Bay. The results for the project (The area enclosed by the project is four thousand hectares, See Fig. 6) are presented in this paper.

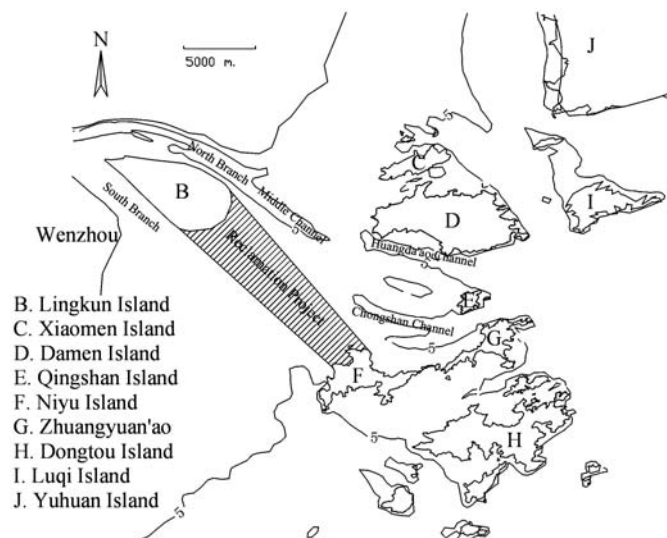


Fig. 6 Sketch of reclamation project

7.1 IMPACT OF THE PROJECT ON TIDAL WATER THROUGHPUT THROUGH SOUTH AND NORTH PORTS OF LINGKUN ISLAND

The tidal volumes through Qili section, Haisi cross section and Huanghua section in the absence or presence of the project are listed in Table 3. The volume of ebb tide through Qili section after the completion of the project is 1.3% less than that in the absence of the project, while the volume of flood tide is 0.7% more; the volume of ebb tide through Haisi section after the completion of the project is 4.2% more, whereas 2.9% ($200-450 \times 10^4 \text{ m}^3$) less for flood tide. The impact of the project is that the flood tide volume through Huangda'ao section is reduced by 15.6% , while the ebb tide volume is reduced by only 3.5%.

Table 3 Tidal water throughput in absence and presence of the project (10^6 m^3)

| Cross Section | North Branch | | South Branch | | Huangda'ao | |
|----------------------------------|--------------|------------|--------------|------------|------------|------------|
| Volume of | Ebb tide | Flood tide | Ebb tide | Flood tide | Ebb tide | Flood tide |
| Tidal range (m) | 5.50 | 5.54 | 5.50 | 5.54 | 5.50 | 5.54 |
| In the absence of the project | 417.684 | -346.676 | 119.715 | -113.168 | 621.794 | -560.014 |
| In the presence of the project | 349.247 | -355.910 | 124.774 | -109.847 | 599.620 | -472.447 |
| Change | 1.007 | 1.013 | 1.042 | 0.971 | 0.965 | 0.844 |
| Increase (+) or decrease (-) (%) | 0.7 | 1.3 | 4.2 | -2.9 | -3.5 | -15.6 |

7.2 IMPACT OF THE PROJECT ON SEDIMENT CONCENTRATION FIELD INSIDE AND OUTSIDE THE ESTUARY

The computed results show that, after the completion of the project, sediment concentration will decrease slightly in all zones except the Middle channel where sediment concentration will increase slightly during flood tide; suspended load concentration will decrease slightly in all zones except several verticals near the project zone in Huangda'ao section. So the impact of the project on the concentration field of suspended load is negligible (Lu and Li, 2001).

7.3 IMPACT OF THE PROJECT ON THE WATER DEPTH OF NAVIGATION CHANNELS

The bed deformation in coming 6 and 12 years is predicted with the available data for two cases, i.e. in the presence of the project and in the absence of the project, respectively. The difference in bed deformation is induced by the project. The computational result shows that the project has little effect on the bed processes of the Oujiang Estuary (Lu and Li, 2001).

Deposition due to the project will occur mainly in the south ditch of the Chongshan channel and its side bar, the Zhuangyuan'ao deep water zone, and the Huangda'ao channel, and the deposition thickness would be very small. Fig.7 shows the variation of erosion and deposition thickness in channels and harbor areas. The Middle channel and the sand barrier have a tendency of erosion in 1-5 years after the project is carried out, and the thickness ranges from 0.003 to 0.024m. Other channels tend to be in a state of deposition. Five-year deposition thickness is 0.057m for the Huangda'ao channel, 0.065m for the north ditch of the Chongshan channel, 0.16m for the south ditch of the Chongshan channel, and 0.113m for the Zhuangyuan'ao deep water zone.

Bed deposition in channels and flow fields interact in the estuary processes. Relative equilibrium will be reached in about 18 years after the completion of the project (see Fig.10). The thickness in this state can be considered as the final erosion and deposition thickness induced by the project. As far as the thickness of deposition and the reduction of water depth are concerned (Lu and Li, 2001), the impact of the project on the south ditch of the Chongshan channel will be more remarkable, than the impact on the north ditch of the Chongshan channel and the Zhuangyuan'ao deep water zone. The water depth will be reduced by 3.12% in the south ditch of the Chongshan channel. The water depth decreases by 1.15% for the north ditch of the Chongshan channel, 0.81% for the Huangda'ao channel, 1.06% for

the sand barrier, 0.68% for the Middle channel, and 0.8% for the Zhuangyuan'ao deep water zone.

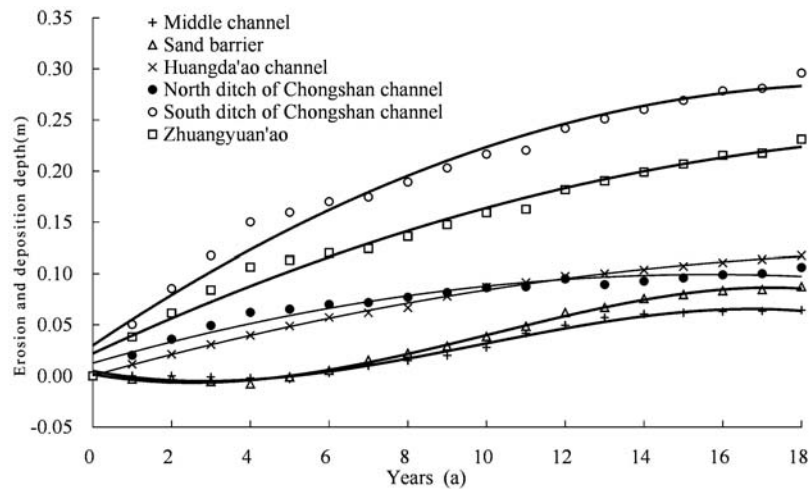


Fig. 7 Erosion and deposition thickness vs. time for different channels after the completion of the project

8. CONCLUSION

(1) The basic principle for the 2D mathematical model of tidal current and sediment transport is given, including the governing equations, initial conditions, boundary conditions, movable boundary technique and computational method. By introduction of the concept of background sediment concentration, the sediment transport capacity formula is obtained. Therefore, a 2D tidal current and sediment mathematical model for the Oujiang Estuary and the Wenzhou Bay is developed.

(2) After several adjustments of the tidal level on the sea boundary, a tidal current field similar to the prototype is obtained. The computed tidal levels are in good agreement with the observed ones at the 18 tidal level stations, and the computed flow velocities and directions also agree well with the field data along the total 52 verticals distributed over the Yueqing Bay, the outfall of the Yueqing Bay, Huangda'ao, the Wenzhou shoal, North Branch, South Branch, Qili, Haisi, Longwan, and Huanghua. The computed tidal discharge hydrographs for the Huangda'ao section are very close to the field observed ones.

(3) According to the computed results of the movable bed, the riverbed deformation in the reaches from Yangfushan to the outfall and outside the Estuary are in good agreement with the observed data in both distribution and quantity. The results imply that the generalization of the runoff, the treatment of boundary conditions, and the selection of coefficients are all reasonable. Therefore, the model developed can be applied to the prediction of bed deformation for the Oujiang Estuary and the Wenzhou Bay.

(4) The model has been used to predict the changes of tidal discharge, velocity field, sediment concentration, and bed deformation resulting from the reclamation project at the Wenzhou shoal. The computational results can be used for decision making of the project.

REFERENCES

- Barber, R. W. 1992. Solving the Shallow Water Equations Using a Non-orthogonal Curvilinear Coordinate System, *Proc. 2nd Int. Conf. on Hydr. And Envir. Modeling of Coast., Estuarine and River Waters*, U.K., 1, 469-480
- DOU Guoren, 2000. Incipient Motion of Sediment Under Currents. *China Ocean Engineering*, 14(4): 391-406
- DOU Guoren, 2001. Similarity Theory of Total Sediment Transport Modeling for Estuarine and Coastal Regions, *J. of Hydro-science and Engineering*, (1):1-12(in Chinese)

- DOU Xiping, LI Tilai and DOU Guoren, 2000. Numerical Model of Total Sediment Transport in the Yangtze River Estuary, *Proceedings of Korea-China Conference on Port and Coastal Engineering*, September 21-23, Korea.
- Holly, F. M. Jr and Rahuel J. L. 1990. Numerical Physical Framework for Mobil-bed Modelling, *J. Hydraulic Research*, 28(4): 401-416.
- HU Kelin, DING pingxing, ZHU shouxian and CAO Zhenyi, 2000. 2-D Current Field Numerical Simulation Integrating Yangtze Estuary with Hangzhou Bay, *China Ocean Engineering*, 14(1):89-102.
- HU Shaoling and S. C. Kot, 1997. Numerical Model of Tides in Pearl River Estuary with Moving Boundary, *Journal of Hydraulic Engineering*, ASCE, 123(1)
- Johnson, B. H. 1980. VAHM-A Vertically Averaged Hydrodynamic Model Using Boundary-fitted Coordinates, MP HL-80-3, U. S. Army Engineer Waterways Experiment Station, Vicksburg, Miss.
- LI Haolin and ZHONG xiecheng, 2001. *Fluvial Process of Oujiang Estuary*, Res. Rep. of Nanjing Hydraulic Research Institute.(in Chinese)
- LU Yongjun and LI Haolin, 2001. 2-D Tidal Current and Sediment Mathematical Model of ining project in Wenzhou shoals, *Res. Rep. Nanjing Hydraulic Research Institute.*(in Chinese)
- LU Yongjun, 1998. Study and Application of Sediment Mathematic Model in Waterway Engineering, Ph.D. Dissertation, Hohai University, Nanjing (in Chinese)
- LU Yongjun, CHEN Guoxiang and Xie Linfong, 1998. A new 2-D sediment model. *River Sedimentation Theory and Application* edited by A.W. Jaywardena, J.H.W. Lee & Z.Y. Wang, 783-788.
- Muslim Muin and Malcolm Spaulding, 1996. Two-Dimensional Boundary-Fitted Circulation Modeling In Spherical Coordinates, *Journal of Hydraulic Engineering*, ASCE, 122(9), September
- Rahuel J. L., Holly, F. M. Jr, Chollet, J.P., Belleudy, P.J. and Yang, G.. 1989, Modeling of Riverbed Evolution for Bedload Sediment Mixtures, *J. Hydraulic Engineering*, ASCE, 115(11):1521-1542.
- SHENG, Y. P. 1986. Numerical Modeling of Coastal and Estuarine Process Using Boundary-fitted Grids, *In 3rd Int. Symp. On River Sedimentation*, 1426-1442.
- Spaulding, M. L., Bedford, K., Blumberg, A., Cheng, R., and Swanson, C., eds., 1994. Estuarine and Coast., modeling III, *Proc. 3rd Int. Conf., ASCE Wtrwy., Port, Coast., and Oc. Div.*, New York.
- TANG Chunbeng, 1963. Incipient Motion of Sediment. *J. of Hydraulic Engineering*, (in Chinese)
- Willemse, J. B. T. M., Stelling, G. S., and Verboom, G. k. 1985. Solving the Shallow Wwater Equations with an Orthogonal Coordinate Transformation. *Int. Symp. on Computational Fluid Dyn.*, Delft Hydr. Communication No. 356, Jan. 86, Delft Hydraulics Laboratory, Delft, The Netherlands